Available online at www.sciencedirect.com
SCIENCE DIRECT®
Polymer 44 (2003) 7625–7634
polymer
www.elsevier.com/locate/polymer

Artificial opals prepared by melt compression

T. Ruhl, P. Spahn, G.P. Hellmann*

Deutsches Kunststoff-Institut (DKI), Schlossgartenstrasse 6, D-64289 Darmstadt, Germany

Received 27 May 2003; received in revised form 24 September 2003; accepted 24 September 2003

Abstract

In recent years, colloidal crystals with a refractive index varying periodically on the scale of the light wavelengths have been prepared by various methods. These photonic crystals reflect light and exhibit, at sufficiently strong contrast, even a complete band-gap in which light cannot propagate in any direction. Most studies published so far were aimed at such high-contrast photonic crystals with a complete band-gap or their precursors. Frequently, a face-centered cubic (fcc) lattice was built up from monodisperse polymer or silica spheres with diameters in the submicron range. Methods as sedimentation and drying of dispersions led to usually small and thin specimens. This report deals with films that were produced by a novel technique based on shear flow in the melts of polymer core-shell latex spheres. The process is fast and yields large area films, thin or thick, in which the latex spheres are crystallized in fcc order. The refractive index contrast of these purely polymeric films is too small for a complete band-gap photonic crystal, but the films are attractive color materials showing wavelength and angle dependent reflection colors.

Keywords: Photonic crystals; Opals; Emulsion polymerisation

1. Introduction

Colloidal crystals, built up by units on the diameter scale 0.2–2 μm, scatter IR or visible light wavelength selectively, according to Braggs law, just as crystals of atoms scatter X-ray or electron radiation. This gives rise to attractive color effects. At sufficiently high refractive contrast, the Bragg peaks widen to band gaps [1–3]. In colloidal crystals with a complete band gap, light can be confined, guided and controlled like electrons in semiconductors [4,5]. Due to these phenomena, these materials are referred to as photonic crystals.

The conditions for a complete photonic band gap are strict. Only some lattice geometries can yield a complete gap, the refractive contrast must be extreme, and the structure must be void of defects which easily can close the gap [6–8]. Methods to prepare such photonic crystals have been and are being developed [9–16]. Suitable techniques are micromachining [9,10], holographic photolithography [11–14] or colloidal assembly [15,16]. Photonic crystals for long waves, especially for IR or microwave radiation, have been produced by machining and lithography [9,14]. But these techniques meet with difficulties in the submicrometer range of lattice spacings that is needed for photonic crystals reflecting visible light. In this range, the colloidal assembly, i.e. the self assembly of supermolecular objects on the submicroscopic scale, may turn out to be the mechanism of choice [17–24].

For visible light, colloidal crystals with a fcc lattice have been prepared from monodisperse inorganic or polymeric spheres with diameters in this range (nature builds opals with just this structure from silica spheres). The synthesis of such monodisperse inorganic [25] or polymeric [15,26] spheres with diameters on the mesoscopic scale 0.1–1 μm is state-of-the-art. But these spheres are not inclined to crystallize readily. The real problem, therefore, is generating the crystalline opal structure.

So far, artificial opals have been prepared from silica [27–30] or polymer [31–40] spheres by techniques of sedimentation [28,30,41] or drying [27,35–39,42] of dispersions. These methods yield small and thin films on various substrates, <50 μm thick with cm^2 areas. The quality of the crystalline order is often excellent but cracking due to shrinkage during the preparation remains a problem. In attempts to produce complete band-gap

* Corresponding author. Tel.: +49-6151164596; fax: +49-6151292855.
E-mail address: ghellmann@dki.tu-darmstadt.de (G.P. Hellmann).

0032-3861/$ - see front matter © 2003 Elsevier Ltd. All rights reserved.
doi:10.1016/j.polymer.2003.09.047

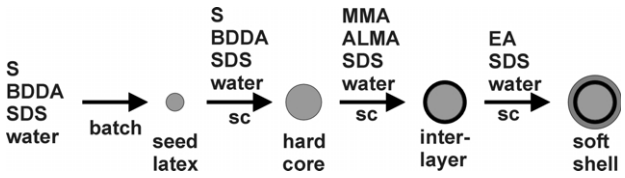

Fig. 1. Synthesis of the latex spheres with a PS core, a PMMA interlayer and a PEA shell.

photonic crystals, these opals are usually inverted by filling the matrix between the spheres with highly refracting inorganics and removing the spheres afterwards [43–46].

In this report, complete band gap crystals are not the primary goal. Polymeric opals from polymer lattices will be discussed, with a low average refractive index and a small contrast. These artificial opals have only incomplete band gaps. Since the average refractive index is so low, the color changes strongly with the angle of light incidence.

Our spheres are synthesized by stepwise emulsion polymerisation. They have a hard–soft architecture with a crosslinked thermoplastic core and an elastomeric grafted-on shell. Owing to the elastomeric shell, these latex spheres form a soft mass at room temperature, which flows easily at elevated temperatures. Film disks with a thickness up to the mm scale and an area on the 100 cm^2 scale were prepared by uniaxial compression molding in which process the spheres were crystallized [47].

While conventional artificial opals have a matrix of air between the spheres, the matrix in our opals consists of the soft shells of the latex spheres which merge during flow in the melt. The hard cores are embedded in this matrix and form the opal lattice. Since the matrix is elastomeric, our films are rubbery and tough.

This paper is supposed to demonstrate the current quality of our photonic crystals. A short introduction was already given in Ref. [47]. Meanwhile, work is in progress to produce opals also by extrusion, injection molding and other techniques of large-scale polymer processing.

2. Experimental

Latex dispersions of thermoplastic-elastomeric core-shell spheres with a polystyrene core (PS), covered by a polymethylmethacrylate (PMMA) interlayer, and a polyethylacrylate (PEA) shell were prepared as described in Ref. [47], by stepwise emulsion polymerisation as indicated in Fig. 1, using sodium dodecylsulfate (SDS) as an emulsifier. The monomers styrene, MMA and EA are increasingly hydrophilic which favors the core-interlayer-shell architecture. The weight composition of all latex spheres was

$$PS_{1/3}PMMA_{1/6}PEA_{1/2}$$

(which means, in terms of radii, $PS_{69}PMMA_{10}PEA_{21}$). The thermoplastic PS-PMMA core was strongly crosslinked, PS with butylendiol diacrylate (BDDA) and PMMA with allyl methacrylate (ALMA), and the PEA shell was grafted onto the PMMA interlayer, more precisely onto the allylic double bond of ALMA. The crosslinking prevents swelling by monomers in consecutive steps and ensures, therefore, the monodispersity of the cores and the entire spheres.

The sphere diameter (150–300 nm) was adjusted by the amount of SDS in the initial batch-step which controls the number of seed particles. Bigger particles result from lower SDS concentrations.

Coagulation of the latex dispersions resulted in an rubbery mass. The elastomeric PEA shells form a continuous

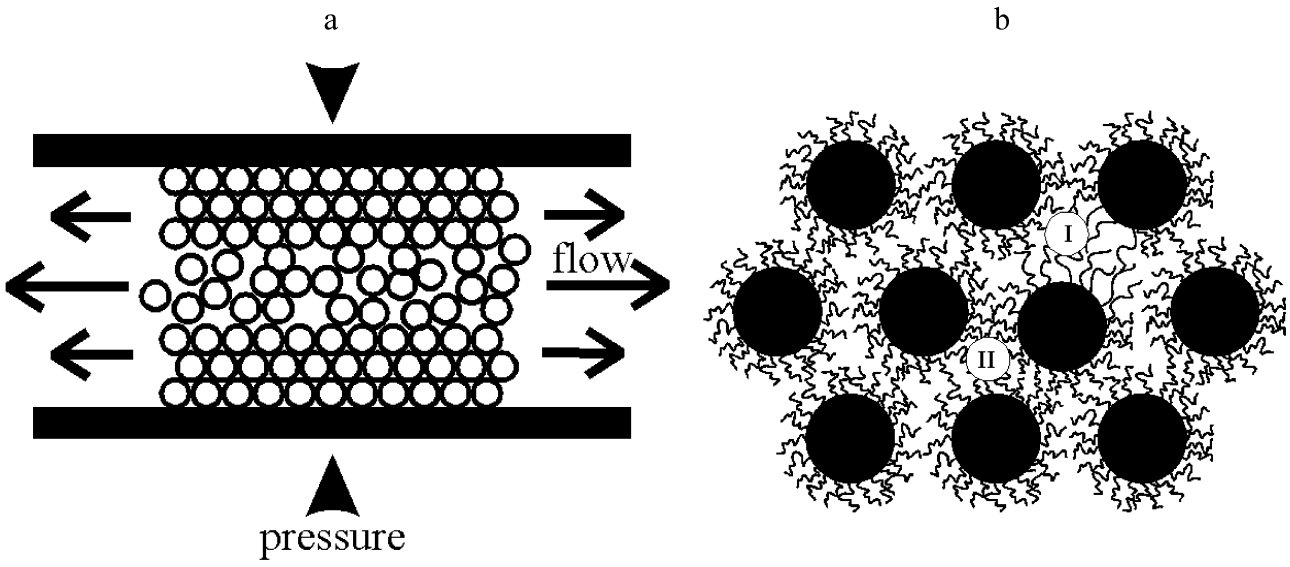

Fig. 2. Preparation of opals from latex spheres: (a) crystallisation of the flowing melt along the plates of the press under uniaxial compression, (b) elastic driving force of the shell chains: around a misplaced core, shell chain coils are compressed on one side (I) and elongated at the other (II); these push the core to its right lattice position.

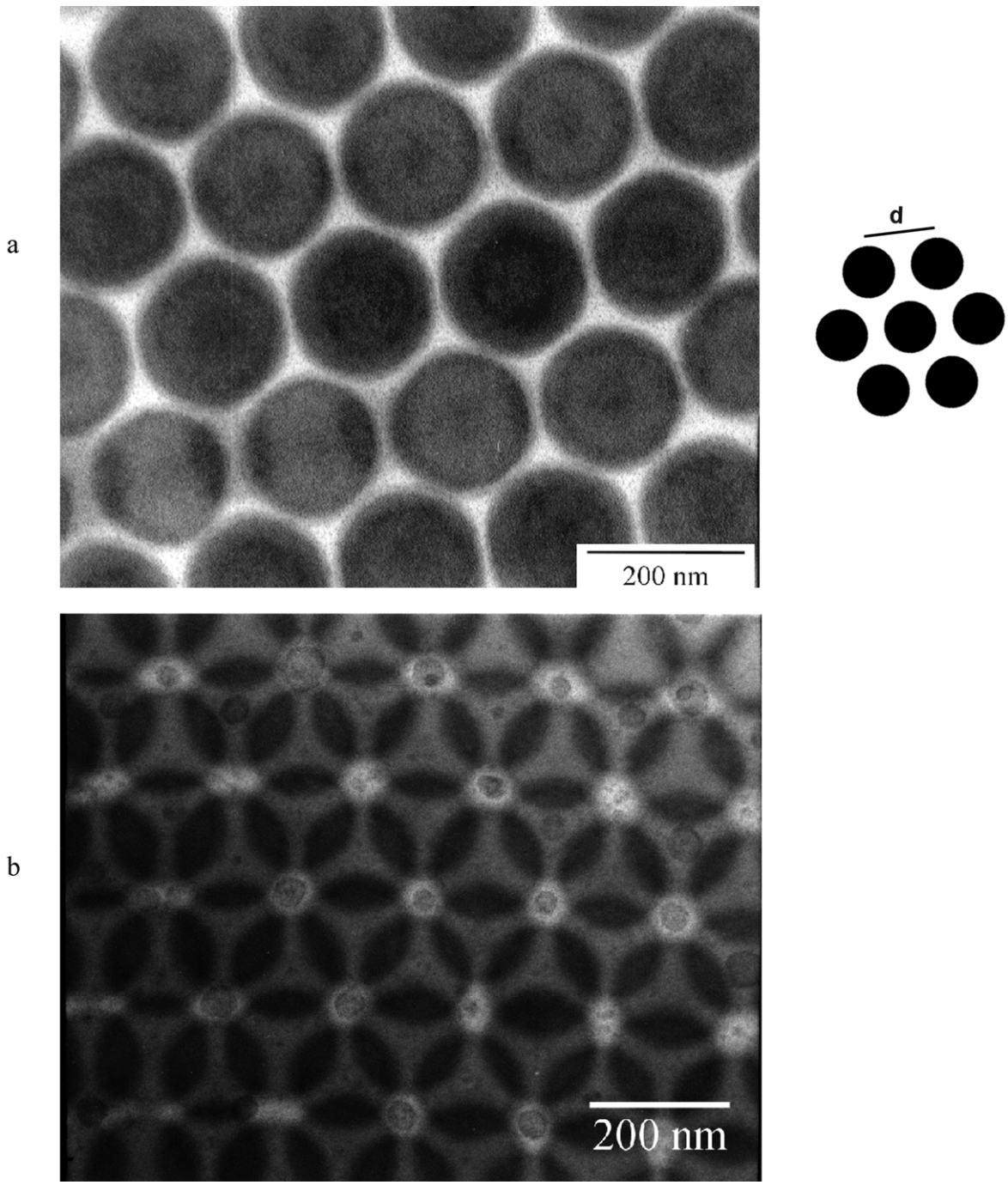

Fig. 3. Opal Ogreen, (111) plane, (a) thin section: one layer. (b) Thicker section: three layers with the ABC order of the fcc lattice (the spheres of the third layer only showing their tips between the spheres of the other two layers).

matrix, in which the crosslinked PS-PMMA cores are dispersed.

This mass was shaped into a cylindric sample (of equal height and diameter) which was uniaxially compressed at 170 °C in a Collin 300 press at 170 °C, with an initial pressure of 1 bar and a final pressure of 50 bar. As indicated in Fig. 2, vertical compression leads to radial horizontal flow. The final product was a round film disk, typically 0.1–0.3 mm thick, with a diameter of about 10 cm. During the flow, the crystalline order grows in the film from the surface inwards. A first crystalline layer is deposited on the plates of the press, and the crystalline order grows then, one layer on top of the other, towards the center layer of the film. The local order in the crystalline layers is probably further improved by the entropic coil elasticity of the shell chains [48] as illustrated by Fig. 2(b) (see Section 2.1).

The architecture of the spheres must satisfy certain conditions: (i) the spheres must be monodisperse in size,

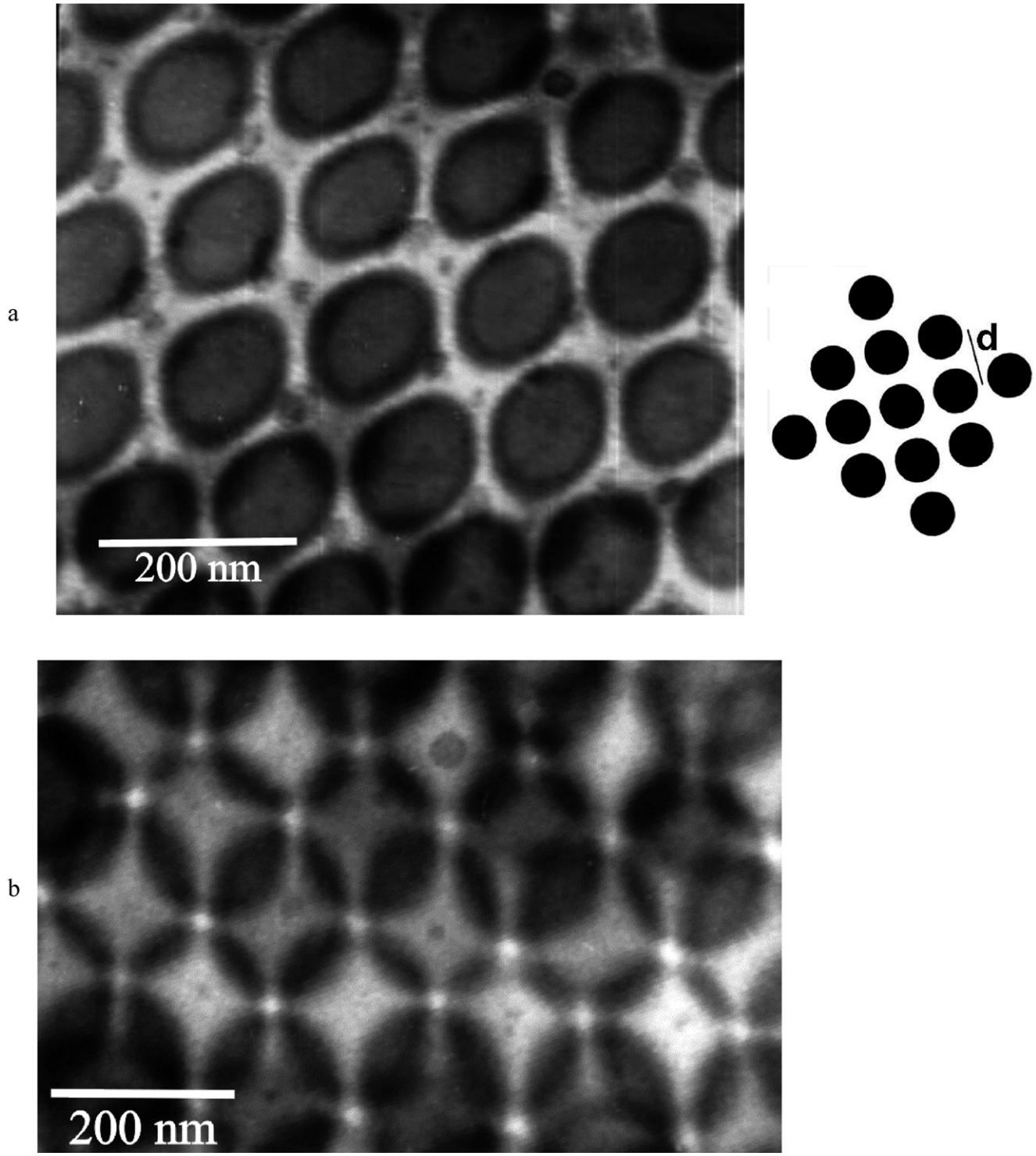

Fig. 4. Opal Ogreen, (200) plane, (a) thin section: one layer. (b) Thicker section: three layers (the spheres of the third layer only showing their tips right under the spheres of the first layer).

(ii) the cores must be crosslinked to preserve their shape in the flowing melt, (iii) most chains of the shell must be grafted onto the core, for which the PMMA interlayer is indispensable, (iv) the elastomeric shell must be thick enough to permit flow in the melt but thin enough to be efficiently grafted. Grafting is particularly important. Films from spheres with weakly grafted shells or films from blends of well-grafted latex spheres with not grafted homopolymer PEA never yielded crystalline order, during melt compression.

UV/Vis spectra were measured in transmission and reflection, in the wavelength range 400–800 nm, using film strips cut from the sample disks as radial sectors. Electron

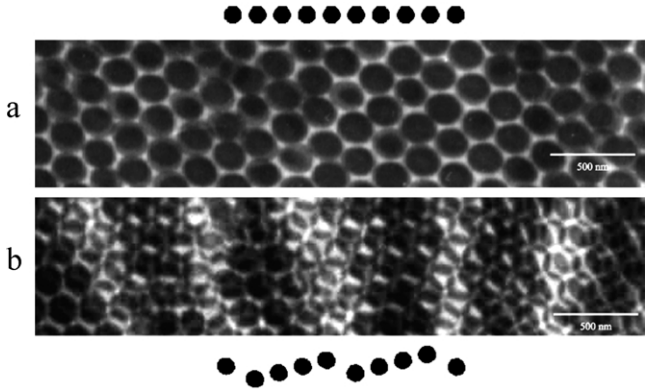

Fig. 5. The (111) plane, cut (a) exactly in one layer and (b) at a slight angle which produces terraces.

micrographs were taken from ultrathin sections prepared at cryo temperatures and stained with RuO_4 which darkens the styrene cores. X-ray scattering at extremely small angles (SAXS) was performed at DESY (Hamburg) using Synchrotron radiation of 0.15 nm wavelength. The particle size distribution was measured with packed column hydrodynamic chromatography using a PL-PSDA particle size distribution analyser from Polymer-Laboratories.

2.1. The fcc lattice and light

The unit cell of the fcc lattice comprises four spheres, all in the next-neighbor distance d, one at the origin and three in the faces. The latter three define the (111) plane which always runs *parallel to the surface* in the films. The spacing is

$$a_{111} = d\sqrt{\frac{2}{3}} \tag{1}$$

In fcc crystals from hard spheres, the next-neighbor distance d in the lattice is equal to the diameter D of the spheres. But not in fcc crystals of our latex spheres. The soft shells of our latex spheres are deformed in the lattice, in order to fill the

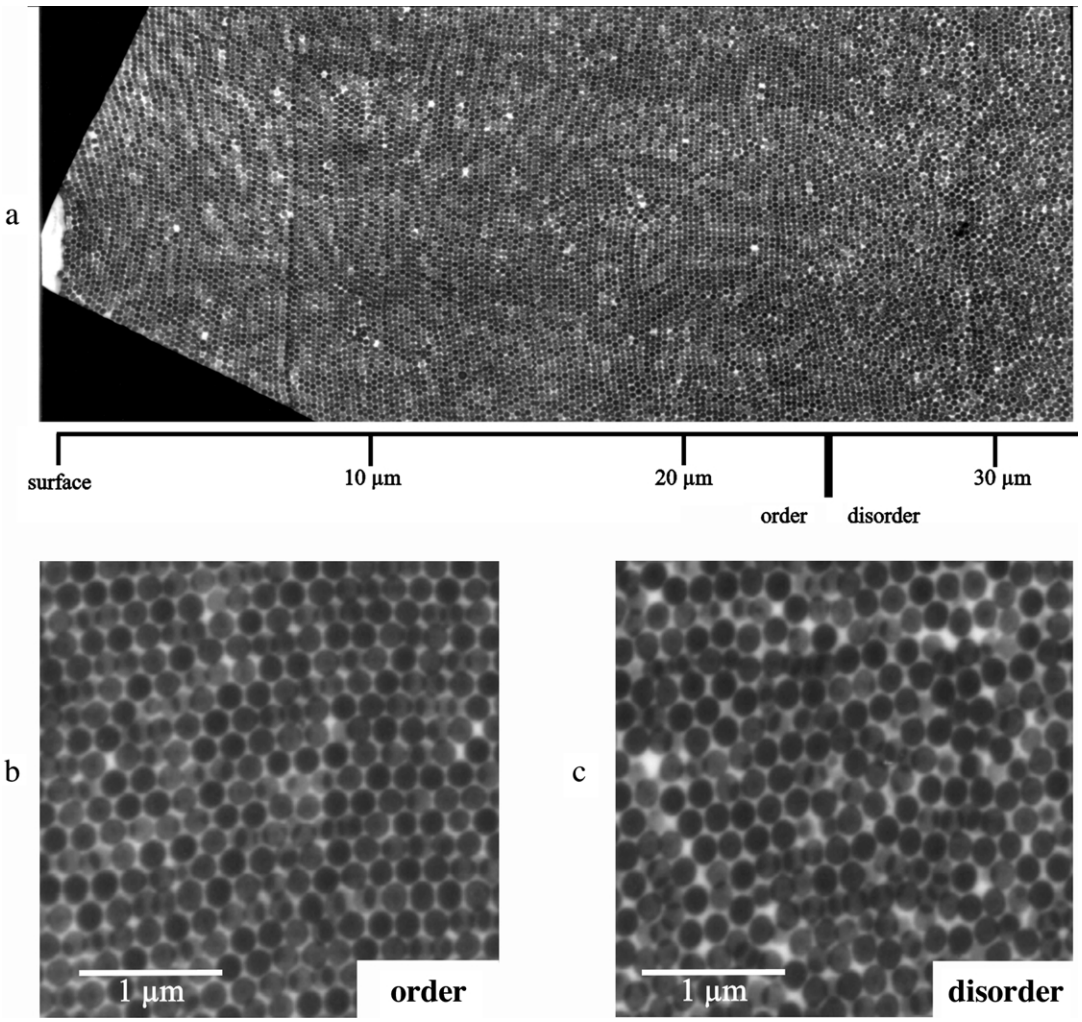

Fig. 6. Order in the opal film Ogreen: (a) overview of the order through the film from the surface, with magnifications (b) of the crystalline layer closer to the surface and (c) the amorphous layer in the center of the film (the order–disorder transition is indicated in (a)).

space between the cores completely. Therefore, the distance d is a bit shorter than the diameter D:

$$d = D\sqrt[3]{\frac{\pi}{3\sqrt{2}}} \tag{2}$$

Other important (hkl) planes in the fcc lattice are three planes each of the types (220), (200) and (−111) at specific angles φ_{hkl} with the film surface, and three planes of the (−220) type at a right angle to the surface. The spacings a_{hkl} and angles φ_{hkl} are given by

$$a_{hkl} = d\sqrt{\frac{2}{h^2+k^2+l^2}} \tag{3}$$

$$\cos\varphi_{hkl} = \frac{h+k+l}{\sqrt{3(h^2+k^2+l^2)}}$$

Light of the wavelength λ_1 (in air), entering the opal at an angle θ, is refracted and travels in the opal at the wavelength λ_n in a direction given by the angle δ. Both are controlled by the average refractive index n_{eff} of the opal:

$$n_{\text{eff}} = \sum \phi_i n_i = \frac{\lambda_1}{\lambda_n} = \frac{\cos\theta}{\cos\delta} = 1.51 \tag{4}$$

where ϕ_i denotes the volume fractions. The value for our films results from those of the core ($n_{\text{PS}} = 1.591$), the interlayer ($n_{\text{PMMA}} = 1.490$) and the shell ($n_{\text{PEA}} = 1.469$) of the latex spheres.

The wavelength (in air) of light reflected by the (111) plane is given by the Bragg equation

$$\lambda_{111}(\theta) = 2n_{\text{eff}}a_{111}\sin\delta = 2a_{111}\sqrt{n_{\text{eff}}^2 - \cos^2\theta} \tag{5}$$

$$\lambda_{111}^{\max} - \lambda_{111}^{\min} = \left(1 - \sqrt{1 - \frac{1}{n_{\text{eff}}^2}}\right)\lambda_{111}^{\max} \cong 0.25\lambda_{111}^{\max}$$

where $\lambda_{111}^{\min}$ and $\lambda_{111}^{\max}$ refer to light entering the opal practically parallel ($\theta \cong 0°$) and vertical ($\theta = 90°$) to the surface. Wavelengths in the window ($\lambda_{111}^{\max}, \lambda_{111}^{\min}$) are reflected. An opal which is red when viewed vertically shows the whole spectrum at decreasing angles and turns finally blue.

3. Results and discussion

Our films are soft but tough enough for the preparation of ultrathin sections for the electron microscopic analysis of the internal structure.

In the following figures, a green opal film (*Ogreen*) is described in detail. The section parallel to the film surface in Fig. 3 shows the PS cores arranged in the PEA matrix in the hexagonal fashion of the (111) plane. A thicker section in Fig. 3(b) proves that the lattice is indeed of the fcc type: it shows three layers, all in a staggered position. In a hexagonal lattice, the third layer would have been eclipsed with the first.

In Fig. 4, electron micrographs of a section through the

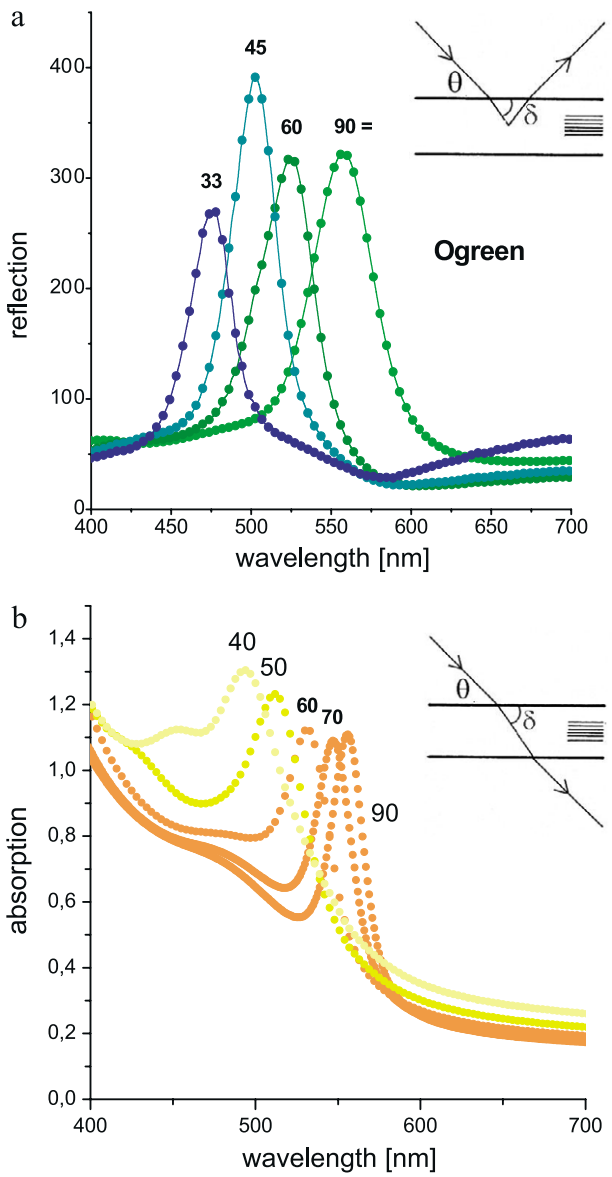

Fig. 7. UV/Vis spectra of the opal Ogreen, measured (a) in reflection, (b) in transmission, as a function of the angle θ of light incidence.

film are shown, along the (200) plane which forms one of the faces of the unit cell. The thicker section in Fig. 4(b) shows the third layer eclipsed with the first, as it must be.

The quality of order was explored with overview electron micrographs at low magnification of extended sections through the film, cut in the thickness direction. Preparing these sections is tedious work: firstly, the exact direction of the *hkl* planes in the film is not known (except that of the (111)), secondly, it is difficult to cut with an ultramicrotome exactly in a desired direction. There is some trial and error. An effect occurring frequently is illustrated by Fig. 5. A section running perfectly along a crystallographic plane shows just one layer (Fig. 5(a)) while a section that happens to run at a slight angle to it crosses stepwise several layers (Fig. 5(b)).

The overview in Fig. 6 displays the order inside the film. The section was cut vertically through the film where the (−220) plane is expected which features somewhat distorted hexagons. Fig. 6(a) demonstrates that the crystalline order is good in more than 100 layers through the film from the surface. Then it falters. This particular film was 100 μm thick and crystalline in approximately 25 μm at each surface. The center half was less or not ordered. Other films yielded crystalline surface layers 30–40 μm thick but a disordered center remained in all cases.

This order–disorder–order sandwich structure through the film suggests the mechanism of the crystallisation illustrated by Fig. 2(a): during the flow of the latex melt under uniaxial compression, crystalline layers of the spheres are constantly being deposited along the plates of the press, one on top of the other. The order thus grows from the plates into the film. Since the melt keeps flowing throughout this process, there will always be a center layer remaining disordered.

The crystalline order is most probably aided by the polymer coil elasticity indicated in Fig. 2(b). Misplaced spheres, suffering from elongated and compressed shell chains, will be moved back to the right crystallographic position.

Electron micrographs were taken at all radii of the disk, in all depths of the film and in all angles. The conclusion from this analysis was that the fcc lattice prevails everywhere. Yet, the crystalline order is not perfect. Defects are visible in Fig. 6, and the crystal layers are not entirely straight. In some electromicrographs, the PS cores appear deformed but this is probably mostly an artifact: the spheres are always compressed in the direction of cutting when the ultrathin sections are prepared [15,49,50].

The optical properties of the opal film *Ogreen* were characterized by UV/Vis spectroscopy. In reflection, the film was green when viewed vertically, turning blue at small angles. In transmission, it was orange, turning yellow at small angles. The UV/Vis spectra are displayed in Fig. 7. At vertical light incidence, the peak yields a spacing of $a_{111} = 183$ nm corresponding to a next-neighbor distance of $d = 225$ nm (Eq. (1)) and a sphere diameter of $D = 248$ nm (Eq. (2)) while the size analysis of the latex dispersion yielded $D = 255$ nm (hydrodynamic fractionation). The fit of Eq. (5) to the angle dependant peak positions in Fig. 7 is satisfactory (Fig. 8).

In transmission, (Fig. 7(b)), not only the peak is observed but also a fairly strong background extinction at wavelengths shorter than the peak. This background is equally

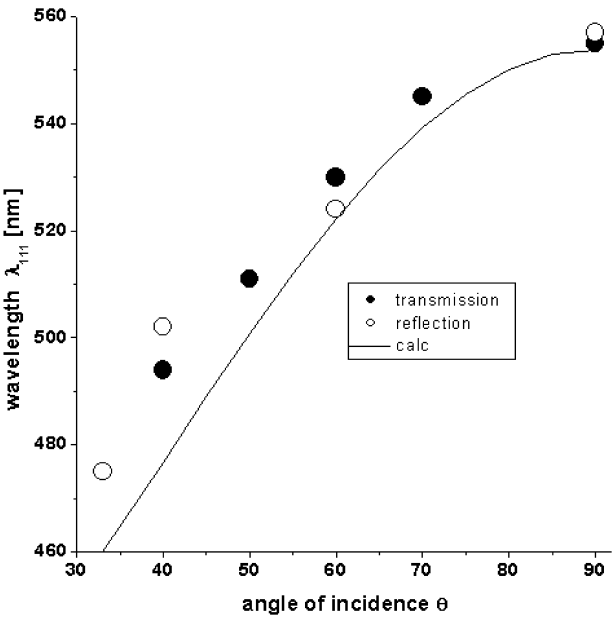

Fig. 8. Peak maxima $\lambda_{111}(\theta)$ from Fig. 6 and fit of Eq. (5) with the spacing $a_{111} = 183$ nm.

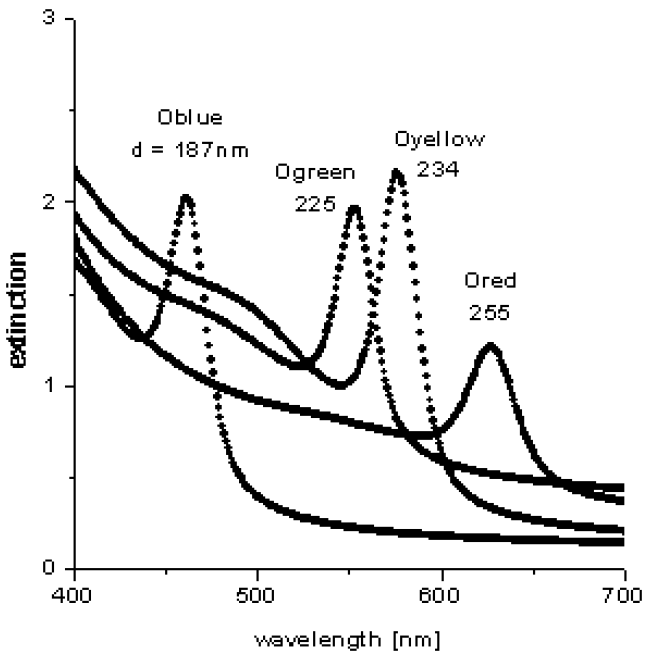

Fig. 9. Opal films of latex spheres differing in diameter, UV/Vis in transmission (next-neighbor distance d by Eqs. (1) and (5), $\theta = 90°$).

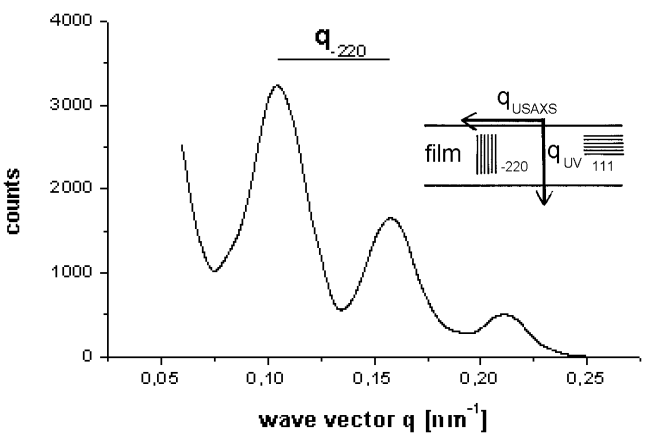

Fig. 10. Ultrasmall angle X-ray scattering (USAXS) curve of the opal Ogreen, measured at vertically incident light and, therefore, probing the (−220) plane, wave vector $q = q_{USAXS}$.

a

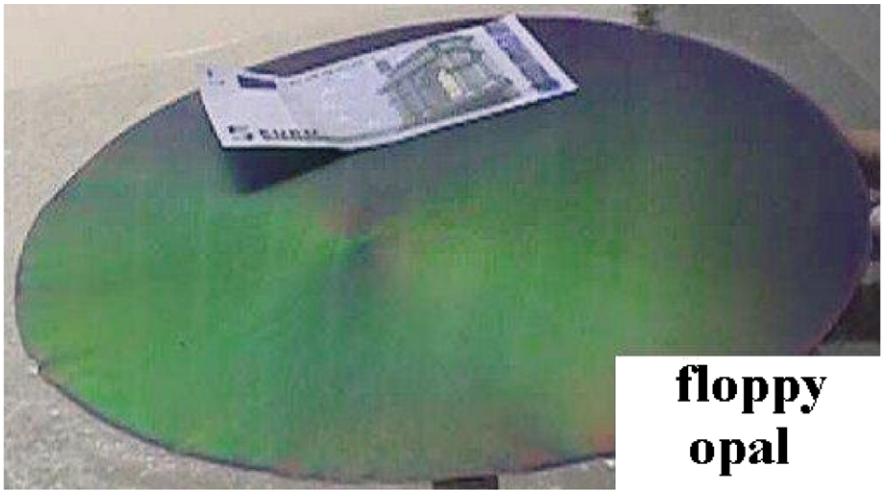

b

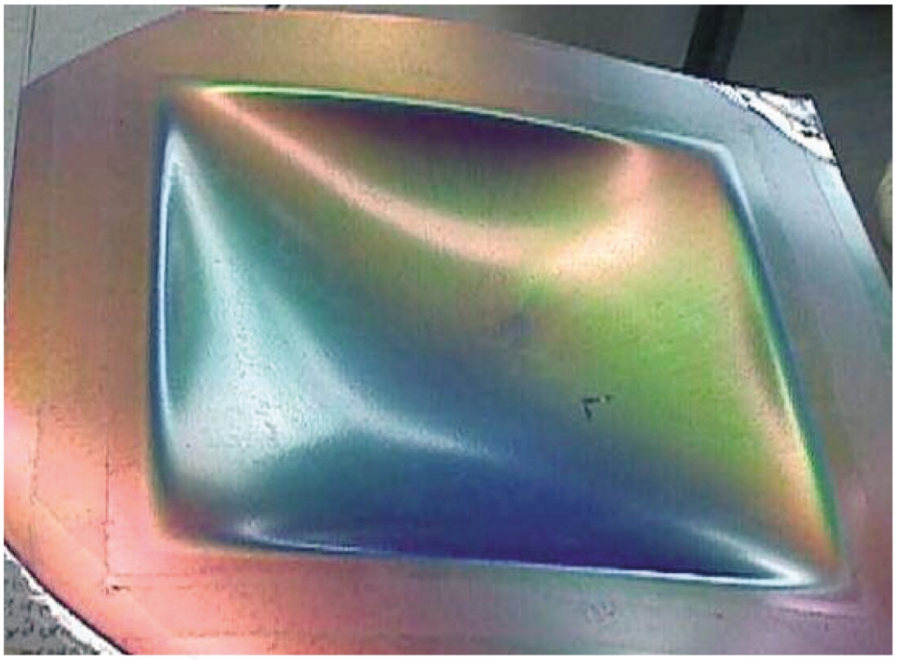

c

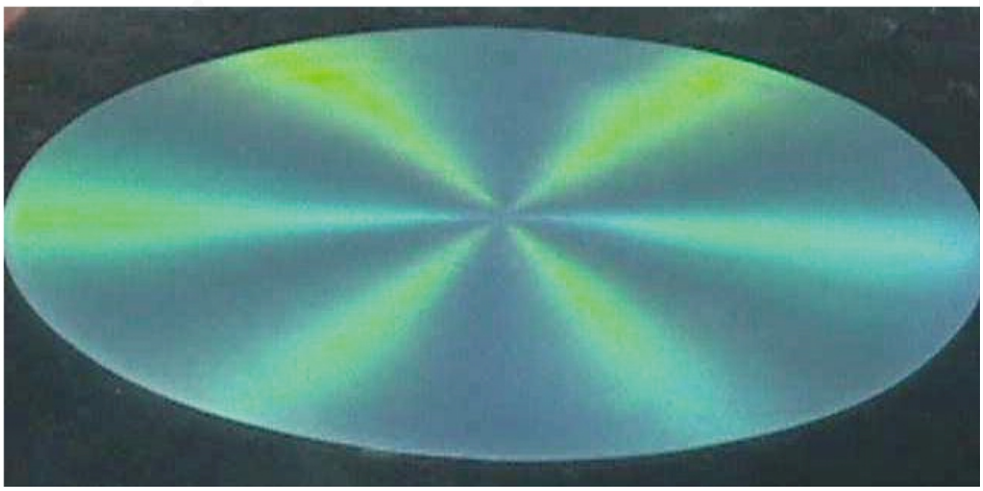

Fig. 11. Opal films: (a) Ogreen (with a 5€ bill, to indicated the size of the film), (b) Ored on a polycarbonate relief foil and (c) an opal film from very large latex spheres which reflects light only in six radial sectors, due to reflection from planes of the (220) family.

observed in latex films which are amorphous [47], so it may be due to the disorder in the center layer of the films. However, even crystalline opals of an excellent quality described in the literature exhibit a similar extinction as well so there may be also a contribution of multiple scattering.

Opal films of all colors were prepared by melt compression from latex spheres varying in diameter. The transmission UV/Vis spectra in Fig. 9 show opals looking blue, green, yellow or red in reflection and with the respective complementary color in transmission. The peak of *Ored* is fairly broad, due to inferior monodispersity of the spheres. The width of the other peaks agrees well with that of colloidal-crystals prepared by other techniques [15,31–40].

In this study, (*hkl*) planes other than the (111) plane were not detected by the UV/Vis spectra, because the spacings a_{hkl} of these planes are too small and their angles φ_{hkl} too steep (Eq. (3)). UV/Vis spectra showing these planes will be the object of the next report which will deal with particularly big latex spheres.

The (−220) plane of the opal *Ogreen* was detected with X-ray scattering at ultrasmall angles (USAXS). As indicated in Fig. 10, UV/Vis and USAXS probe different wave vectors q (q_{UV} and q_{USAXS}): when a film is irradiated with a beam perpendicular to the surface, UV measures back reflection (180°, q_{UV}) from the (111) plane parallel to the surface while USAXS measures forward scattering (<1°, $q_{-220} = q_{USAXS}$) from the (−220) plane which extends at right angles to the surface. The curve in Fig. 10 shows the 2nd–4th order of the (−220) plane, the wave vector q_{-220} corresponding to the distance between peaks. This yields a next-neighbor distance d in good agreement with the UV/Vis peak for *Ogreen* in Fig. 9:

$$d = 2a_{-220} = \frac{4\pi}{q_{-220}} = 237\ \text{nm} \quad (6)$$

Work is in progress on opal films from particularly large latex spheres where, besides the (111) plane, several other (*hkl*) planes can be investigated.

In Fig. 11, the color effects of our latex films are demonstrated. The opal *Ogreen* exhibits an even green color due to reflection from the (111) plane. The opal Ored, being attached to an uneven polycarbonate substrate, shows all colors of the spectrum, depending on the angles. The film in Fig. 11(c), finally, is a first product of the current research on lattices with very large spheres. The (111) reflection is shifted into the IR region, and visible is only a reflection from the three planes of the (220) family. That this reflection is confined to six radial sectors seems to indicate that the fcc lattice in these films is, in fact, macroscopically oriented.

Acknowledgements

We thank Merck KGaA (Darmstadt, Germany) for financial support. We also would like to thank A. Kastner and I. Alig (DKI) for the USAXS measurements and F. Schael (Institute for Chemistry, University of Potsdam) for the UV/Vis spectra in reflection.

References

[1] Yablonovitch E. Phys Rev Lett 1987;58:2059.
[2] John S. Phys Rev Lett 1987;58:2486.
[3] Joannopoulos JD, Meade RD, Winn JN. Photonic crystals —molding the flow of light. Princeton: Princton University Press; 1995.
[4] Joannopoulos JD, Villeneuve PR, Fan S. Nature 1997;386:143.
[5] van Blaaderen A. MRS Bull 1998;23(10):39.
[6] Busch K, John S. Phys Rev E 1998;58:3896.
[7] Yablonovitch E. Scientific American 2001;9:47.
[8] Li ZY, Zhang ZQ. Adv Mater 2001;13:433.
[9] John S. In: Soukoulis CM, editor. Photonic bandgap materials. Dortrecht/Boston/London: Kluwer Academic Press; 1995.
[10] Noda S. Physica B 2000;279:142.
[11] Campbell M, Sharp DN, Harrison MT, Denning RG, Turberfield AJ. Nature 2000;404:53.
[12] Krauss T, Song YP, Thoms S, Wilkinson CDW, De La Rue RM. Electron Lett 1994;30:1444.
[13] Cumpston BH, Anathavel S, Barlow S, Dyer DL, Ehrlich JE, Erskine LL, Heikal A, Kuebler SMS, Lee IY, McCord-Maughon D, Qin J, Röckel H, Rumi M, Wu XL, Marder SR, Perry JW. Nature 1999;398:51.
[14] Birner A, Wehrspohn RB, Gösele UM, Busch K. Adv Mater 2001;13:377.
[15] Fitch RM. Polymer colloids—a comprehensive introduction. San Diego: Academic Press; 1997.
[16] Pieranski P. Contemp Phys 1983;24:25.
[17] Asher SA, Holtz J, Weissmann J, Pan G. MRS Bull 1998;23:44.
[18] van Blaaderen A, Wiltzius W. Adv Mater 1997;9:833.
[19] Yang P, Rizvi AH, Messer B, Chmelka BF, Whitesides GM, Stucky GD. Adv Mater 2001;13:427.
[20] Xia Y, Gates B, Yin Y, Lu Y. Adv Mater 2000;12:693.
[21] Vlasov YA, Astratov VN, Baryshev AV, Kaplyanskii AA, Karimov OZ, Limonov MF. Phys Rev E 2000;61:5784.
[22] Lu Y, Yin Y, Xia Y. Adv Mater 2001;6:415.
[23] Alexander CE, Urbas AM, De Rege P, Chen CX, Swager TM, Hadjichristidis N, Xenidou M, Fetters LJ, Joannopoulos JD, Fink Y, Thomas EL. Adv Mater 2001;13:421.
[24] Urbas A, Sharp R, Fink Y, Thomas EL, Xenidou M, Fetters LJ. Adv Mater 2000;12:812.
[25] Stöber W, Fink A, Bohn EJ. Colloid Interface Sci 1968;26:62.
[26] Hearn J, Wilkinson M, Goodall AR. Adv Colloid Interface Sci 1981;14:173.
[27] Jiang P, Bertone JF, Hwang KS, Colvin VL. Chem Mater 1999;11:2132.
[28] van Blaaderen A. Science 1998;282:887.
[29] Mayoral R, Requena J, Moya JS, Lopez C, Cintas A, Miguez H, Meseguer F, Vazquez L, Holgado M, Blanco A. Adv Mater 1997;9:257.
[30] Peigen N, Peng D, Bingying C, Xinyan L, Zhang D. Adv Mater 2001;13:437.
[31] Tarhan II, Watson GH. Phys Rev Lett 1996;76:315.
[32] Pusey PN, van Mengen W, Bartlett P, Ackerson BJ, Rarity JG, Underwood SM. Phys Rev Lett 1989;63:2753.
[33] Rogach OE, Kornowski A, Kapitaonov AM, Gaponenko NV, Gaponenko SV, Eychmüller A, Rogach AL. Mater Sci Engng B 1999;64:64.
[34] Asher SA, Flaugh PL, Washinger G. Spectroscopy 1986;1:26.
[35] Luck W, Klier M, Wesslau H. Ber Bunsengesellschaft 1963;67:75.

[36] Subramania G, Constant K, Biswas RH, Sigalas MM, Ho KM. Adv Mater 2001;13:443.
[37] Müller M, Zentel R, Maka T, Romanov SG, Sotomayor-Torres CM. Chem Mater 2000;12:2508.
[38] Egen M, Zentel R. Chem Mater 2002;14:2176.
[39] Goldenberg LM, Wagner J, Stumpe J, Paulke BR, Görnitz E. Langmuir 2002;18:3319.
[40] Kumaraswamy G, Dibaj AM, Caruso F. Langmuir 2002;18:4150.
[41] Miguez H, Meseguer F, Lopez C, Blanco A, Moya JS, Requena J, Mifsud A, Fornes V. Adv Mater 1998;10:480.
[42] Luck W, Weslau H. Festschrift Carl Wurster. Ludwigshafen: BASF; 1960. p. 279.
[43] Blanco A, Chomski E, Grabtchak S, Ibisate M, John S, Leonard SW, Lopez C, Meseguer F, Miguez H, Mondia JP, Ozin GA, Toader O, van Driel HM. Nature 2000;405:414.
[44] Blanford CF, Yan H, Schroden RC, Al-Daous M, Stein A. Adv Mater 2001;13:401.
[45] Wijnhoven JEGJ, Vos WL. Science 1998;281:802.
[46] Holland BT, Blanford CF, Do T, Stein A. Chem Mater 1999;11:795.
[47] Ruhl T, Hellmann GP. Macromol Chem Phys 2001;202:3502.
[48] Ishizu K. Macromol Rapid Commun 2003;24:291.
[49] Kim YS. Synthese und Charakterisierung von mehrphasigen polymeren Latices mit Kern/Schale Morphologie. Aachen: Shaker; 1993.
[50] Okubo M, Hosotani T, Yamashita T. Colloid Polym Sci 1996;274:279.